ADVANCES IN ATMOSPHERIC SCIENCES, VOL. 32, JUNE 2015, 783–793

Influence of Positive and Negative Indian Ocean Dipoles on ENSO via the Indonesian Throughflow: Results from Sensitivity Experiments

ZHOU Qian[1,2], DUAN Wansuo*[1], MU Mu[3], and FENG Rong[1]

[1]*State Key Laboratory of Numerical Modeling for Atmospheric Sciences and Geophysical Fluid Dynamics, Institute of Atmospheric Physics, Chinese Academy of Sciences, Beijing* 100029

[2]*University of Chinese Academy of Sciences, Beijing* 100049

[3]*Key Laboratory of Ocean Circulation and Wave, Institute of Oceanology, Chinese Academy of Sciences, Qingdao* 266071

(Received 1 July 2014; revised 10 October 2014; accepted 15 November 2014)

ABSTRACT

The role of the Indonesian Throughflow (ITF) in the influence of the Indian Ocean Dipole (IOD) on ENSO is investigated using version 2 of the Parallel Ocean Program (POP2) ocean general circulation model. We demonstrate the results through sensitivity experiments on both positive and negative IOD events from observations and coupled general circulation model simulations. By shutting down the atmospheric bridge while maintaining the tropical oceanic channel, the IOD forcing is shown to influence the ENSO event in the following year, and the role of the ITF is emphasized. During positive IOD events, negative sea surface height anomalies (SSHAs) occur in the eastern Indian Ocean, indicating the existence of upwelling. These upwelling anomalies pass through the Indonesian seas and enter the western tropical Pacific, resulting in cold anomalies there. These cold temperature anomalies further propagate to the eastern equatorial Pacific, and ultimately induce a La Niña-like mode in the following year. In contrast, during negative IOD events, positive SSHAs are established in the eastern Indian Ocean, leading to downwelling anomalies that can also propagate into the subsurface of the western Pacific Ocean and travel further eastward. These downwelling anomalies induce negative ITF transport anomalies, and an El Niño-like mode in the tropical eastern Pacific Ocean that persists into the following year. The effects of negative and positive IOD events on ENSO via the ITF are symmetric. Finally, we also estimate the contribution of IOD forcing in explaining the Pacific variability associated with ENSO via ITF.

Key words: IOD, Pacific Ocean, ENSO, Indonesian Throughflow

Citation: Zhou, Q., W. S. Duan, M. Mu, and R. Feng, 2015: Influence of positive and negative Indian Ocean dipoles on ENSO via the Indonesian Throughflow: Results from sensitivity experiments. *Adv. Atmos. Sci.*, **32**(6), 783–793, doi: 10.1007/s00376-014-4141-0.

1. Introduction

The El Niño-Southern Oscillation (ENSO) is the most important air–sea interaction phenomenon in the tropical Pacific. The occurrence of ENSO causes extreme weather and climate events across the globe, leading to severe natural disasters (Wang et al., 2000; Diaz et al., 2001; Alexander et al., 2002). Consequently, it is of great importance to study the dynamics of ENSO to predict events successfully (Latif et al., 1998; Chen et al., 2004; Jin et al., 2008; Luo et al., 2008; Tippett et al., 2011).

The Indian Ocean Dipole (IOD) is an air–sea coupled phenomenon. Some studies argue that the IOD is dependent on Pacific Ocean air–sea interactions (Allan et al., 2001; Nicholls et al., 2001; Baquero-Bernal et al., 2002; Lau and Nath, 2003), while others claim it is an intrinsic physical entity, independent of ENSO (Saji and Yamagata, 2003; Behera et al., 2006; Luo et al., 2010). Either way, the IOD can be influenced by ENSO events (Nagura and Konda, 2007; Schott et al., 2009; Luo et al., 2010; Roxy et al., 2011).

It has been suggested that ENSO prediction by both statistical (Clarke and Van Gorder, 2003; Izumo et al., 2010; Izumo et al., 2014) and dynamical models (Luo et al., 2010) is improved by including Indian Ocean information. For example, Izumo et al. (2010) predicted the ENSO peak during 1981–2009 with a lead time of 14 months by adopting the corresponding boreal autumn Dipole Mode Index (DMI) and warm water volume (WWV) as predictors. They also extended this conclusion to ENSO forecasting during 1872–2008 (Izumo et al., 2014), and revealed that the DMI is much more helpful in improving ENSO hindcast skill compared with an Indian Ocean basin-wide mode, the Indian Monsoon, or the ENSO index itself. These results imply that the IOD may significantly influence ENSO predictability. Furthermore, the atmospheric bridge is suggested to be a lead-

* Corresponding author: DUAN Wansuo
Email: duanws@lasg.iap.ac.cn

ing contributor to the influence of IOD on ENSO (Alexander et al., 2002; Annamalai et al., 2005; Kug and Kang, 2006). Gear-like coupling between the Indian and Pacific oceans (GIP) is another mechanism proposed to interpret the interactions between the tropical Indian and Pacific Ocean climate systems (Wu and Meng, 1998). Sensitivity experiments have shown that, through GIP, the air–sea interaction in one ocean basin forced by zonal wind stress anomalies can cause air–sea interaction in the other ocean, resulting in anomalous SST (Meng and Wu, 2000).

By calculating observed time series lag correlations, Yuan et al. (2013) recently suggested that the influence of the IOD on ENSO may occur via the Indonesian Throughflow (ITF), the only ocean channel between the tropical Indian and Pacific oceans. Earlier, they had also conducted GCM sensitivity experiments with a closed atmospheric bridge which, together with the observational results, confirmed their hypothesis (Yuan et al., 2011). The results suggest that it is the ITF that can convey the IOD event forcing into the tropical Pacific Ocean in the following year. However, it is worth noting that Yuan et al. (2011) only studied the influence of one IOD event (in 1997) on the following year's Pacific Ocean air–sea coupled system, and did so using the LASG (State Key Laboratory of Numerical Modeling for Atmospheric Sciences and Geophysical Fluid Dynamics) IAP (Institute of Atmospheric Physics) Climate Ocean Model (LICOM) and a coupled model. Moreover, the 1997 IOD event was an extreme positive event. In this paper, we ask if another ocean model—version 2 of the Parallel Ocean Program (POP2) ocean general circulation model (OGCM)—shows similar connections between positive IOD events and subsequent La Niña-like states. Like ENSO events, IOD events also possess significant asymmetry (Hong et al., 2008a; 2008b). Therefore, we also question how a negative IOD event influences ENSO in the Pacific Ocean: Is it opposite to that of a positive IOD? Also, to what extent does the IOD forcing contribute to the Pacific variability associated with ENSO? These questions are addressed in the present study.

The remainder of this paper is organized as follows. Section 2 describes the model and data used in this study. The experimental strategy is introduced in section 3. The role of the ITF in conveying IOD forcing to the Pacific Ocean is investigated in section 4. The contribution of IOD forcing to the Pacific variability associated with ENSO via the ITF is estimated in section 5, followed by a summary and discussion in section 6.

2. Model and data

The POP2 OGCM (Danabasoglu et al., 2011), originally developed at the Los Alamos National Laboratory, but with more recent work on parameterizations largely added by the

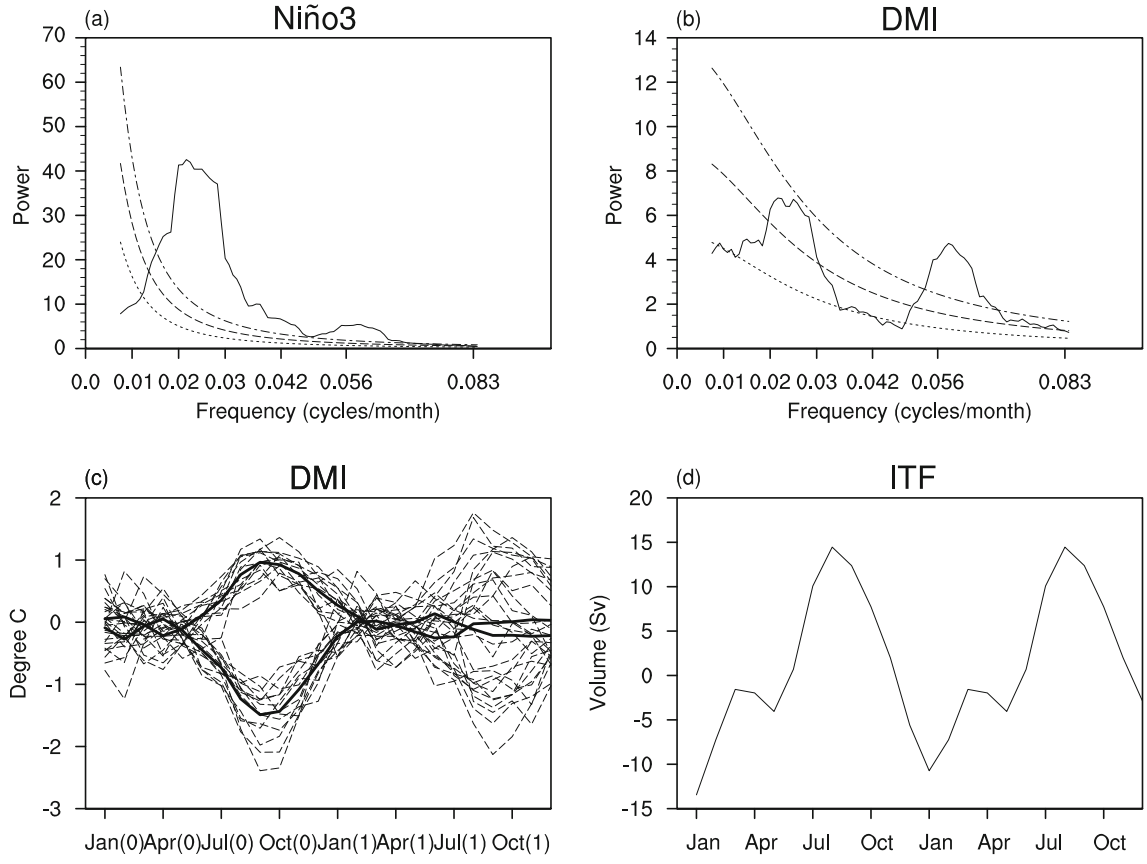

Fig. 1. Simulation of ENSO and IOD in the CESM1.0.3 control run (year 0051–0150). Power spectrum of (a) the Niño3 index and (b) Dipole Mode Index (DMI). (c) Fourteen positive/negative IOD events from the coupled model (dashed lines) (mean shown in bold). (d) Monthly mean climatological ITF transport volume.

National Center for Atmospheric Research, is used in this study. It is a z-level hydrostatic primitive equation model with 60 levels. The vertical spacing is 10 m at the surface and varies with depth. The nominal horizontal resolution is $1^\circ \times 1^\circ$ in the off-equatorial area with an enhanced resolution of $(1/3)^\circ$ latitude by 1° longitude in the tropics.

The observational data used are from version 2 of the Coordinated Ocean Research Experiments (COREv2), with a horizontal resolution of 1.9° (lat) $\times$ 1.875° (lon). The relevant variables include: the atmospheric forcing of precipitation; air absolute humidity; sea level pressure; air temperature; wind speed; and longwave downward, shortwave downward, and shortwave upward radiation. All these forcing data are from the Geophysical Fluid Dynamics Laboratory (GFDL) website (http://data1.gfdl.noaa.gov/nomads/forms/mom4/COREv2.html). Observational sea surface height (SSH) from the TOPEX/Poseidon satellite mission is also used.

Due to the short history of observational records, we additionally use forcing data extracted from a coupled general circulation model's long-term run. Since version 1.0.3 of the Community Earth System Model (CESM1.0.3) (which uses POP2 as its ocean component) simulates both the ENSO (Deser et al., 2012) and IOD well, and provides an acceptable simulation of the ITF (Large and Danabasoglu, 2006; Jochum et al., 2009), we adopt the output of this coupled model to validate the results obtained from the observation. CESM1.0.3 has been integrated for 150 years, and the first fifty years (0001–0050) of the coupled run are discarded due to the initial adjustment of the model. The simulated ENSO in the coupled model has a period of 3–6 years (Fig. 1a), with a reasonable amplitude and latitudinal width of the anomalous equatorial zonal wind stress. El Niño events modeled by CESM1.0.3, like observed ENSO events, also peak at the end of the calendar year. The simulated IOD has a period of 1–2 years (Fig. 1b), usually peaking in boreal autumn and decaying in boreal winter (Fig. 1c), and roughly captures the features of observed IOD events. Because the 6°S section goes through three major channels—the Lombok Strait, the Ombai Strait, and the Timor Sea—the ITF in this study

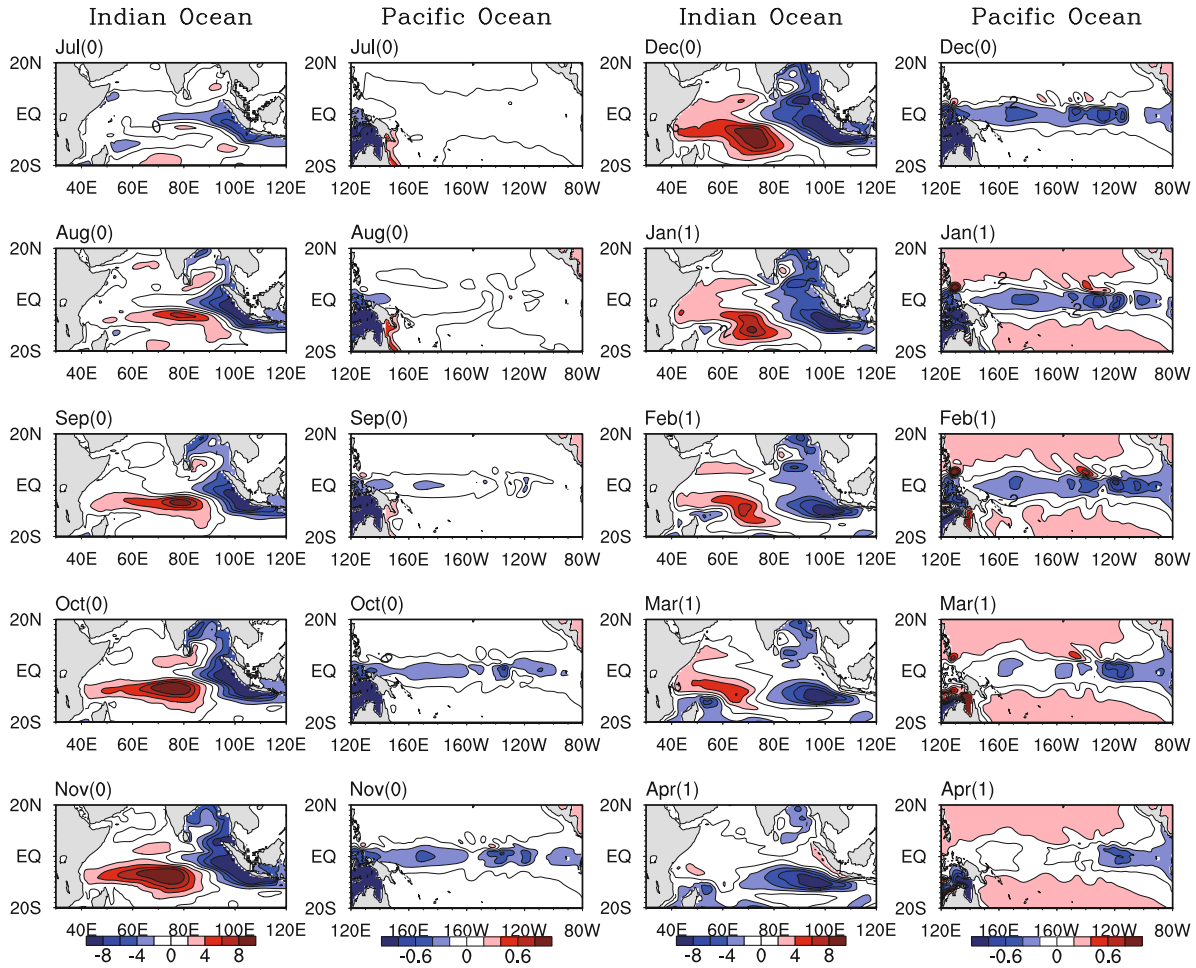

Fig. 2. OGCM-simulated SSHAs between sensitivity runs forced by atmospheric forcing from observed positive IOD events and a control run during Jul(0) to Apr(1) over the Indian Ocean (contour interval: 2 cm) and Pacific Ocean (contour interval: 0.2 cm).

is defined as the flow across the 6°S section from 115°E to 130°E in the upper 700 m of the Indonesian seas. The simulated monthly mean climatology of the ITF transport volume (Fig. 1d) also has a significant seasonal signal, which peaks in summer and decays in winter. This feature is in accordance with other OGCM simulation products (Lee et al., 2010) and observations (Wyrtki, 1987; Meyers et al., 1995; Shinoda et al., 2012). Based on this analysis, we accept that the simulated ENSO, IOD and ITF are suitable for investigating the role of the ITF in connecting the Indian and Pacific oceans.

3. Design of the sensitivity experiments

We use the POP2 OGCM to conduct numerical experiments. The model is first integrated with climatological forcing for 60 years, referred to hereafter as the "control run". Then, sensitivity experiments are conducted at the end of year 57 to replace the Indian Ocean forcing with the daily wind stress and heat flux of an IOD year. The differences between the sensitivity experiments and the OGCM control run thus represent the interannual variations of the Indian Ocean circulation forced by the IOD wind and heat flux anomalies in a non-coupled configuration, i.e. the IOD forcing influences on the Pacific Ocean through the Indonesian passages. In this study, we focus on the differences between the sensitivity experiments and the OGCM control run to explore the role played by the ITF during both positive and negative IOD events in influencing Pacific SST associated with ENSO. For simplicity, we use the term "anomalies" to denote these differences.

For the observational run, the mean atmospheric state (see section 2) during 1970–2000 is used as the climatological forcing. The daily atmospheric forcing associated with the positive IOD years of 1982, 1983, 1991, 1994 and 2006, and the negative IOD years of 1975, 1980, 1981, 1989 and 1992, are used. For the model data, atmospheric data of 14 positive IOD events and 14 negative IOD events from the coupled long-term run of CESM1.0.3 (shown in Fig. 1c) and the mean of 100 years of the control run are used as daily and climatological forcing, respectively.

4. Role of the ITF in conveying the IOD forcing on the Pacific Ocean

First, we compare the POP2 simulations to those of Yuan et al. (2011) in describing the role of the ITF during the 1997 positive IOD event. The sensitivity experiments associated with the 1997 positive IOD event show that it can induce a La Niña-like mode in the following year via the ITF, in good agreement with the results of Yuan et al. (2011) (for brevity, the details are omitted here). Having established this good agreement, we proceed to simulate the role of the ITF in conveying the positive IOD impact on the Pacific SST by conducting more sensitivity experiments with IOD forcing using POP2. In particular, we investigate the role of the ITF in conveying the negative IOD's forcing on Pacific SST.

4.1. *Role of the ITF in conveying the positive IOD forcing on the Pacific Ocean*

4.1.1. *Sensitivity experiments forced by the observed atmosphere during positive IOD events*

First, we use the observed climatological atmospheric state to force the POP2 model, producing a control run. Second, two-year sensitivity experiments are performed using the observed daily heat flux and wind observations from positive IOD years (1982, 1983, 1991, 1994 and 2006) and their following years as the external forcing over the Indian Ocean, whilst at the same time retaining the climatological atmospheric forcing over other ocean basins. The differences between the sensitivity experiments and the control run are obtained as the so-called anomalies, including SSH anomalies (SSHAs) and sea surface temperature anomalies (SSTAs), to identify the role of the ITF in the IOD's influence on the Pacific SST associated with ENSO.

Figure 2 displays the composite SSH anomalies of the observed positive IOD forcing periods over the Indian Ocean and the Indo-Pacific regions from Jul(0) to Apr(1) ("0" and "1" denote the IOD year and the subsequent year, respectively). Positive IODs occur with positive SSHAs in the western Indian Ocean, and negative SSHAs in the east; the nega-

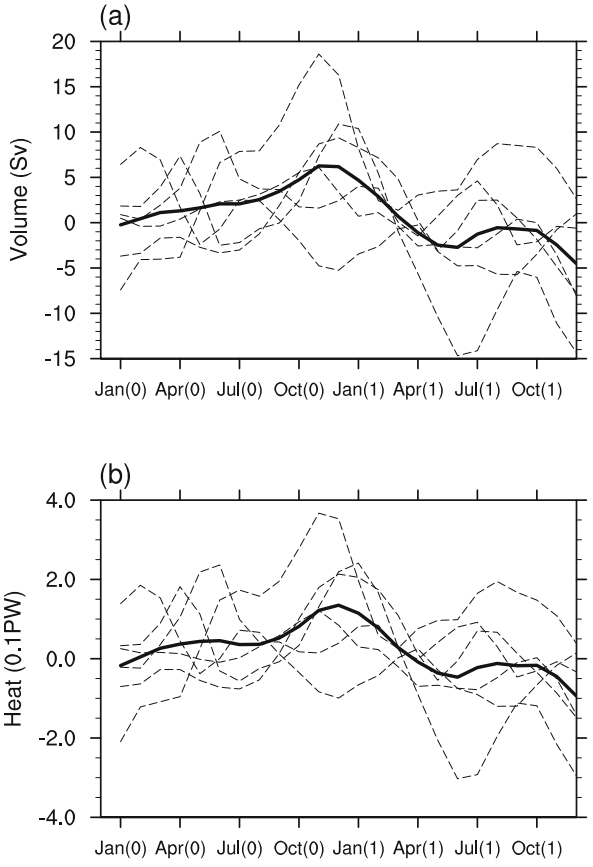

Fig. 3. The ITF anomaly for (a) volume transport and (b) heat flux transport differences between sensitivity experiments of observed positive IOD events and the OGCM control run (dashed lines). Solid bold lines represent the mean.

tive SSHAs in the eastern Indian Ocean indicate a shoaled thermocline and upwelling currents. The upwelling anomalies are amplified and transported into the Pacific Ocean in Aug(0), and persist in the equatorial Pacific Ocean into the following year. The SSHAs indicate that the differences between the sensitivity experiments and the control run arise from the shutting down of the atmospheric bridge while the ITF remains. The resulting propagation of negative SSHAs from the Indian Ocean to the Pacific Ocean demonstrates the role of the ITF in connecting the Indian Ocean and Pacific Ocean interannual anomalies.

The anomalies of ITF volume and heat transport along 6°S are shown in Fig. 3. If the ITF anomalies are positive (negative), it means that the warm pool loses (gains) more heat and WWV to (from) the Indian Ocean, implying a propagation of the cold (warm) temperature anomalies from the Indian Ocean to Pacific Ocean. During positive IOD event years, the ITF anomalies become positive in Aug(0), peak in Dec(0), decay over the winter and reverse to negative in Mar(1). Positive ITF transport anomalies lead to cold sea temperature anomalies in the eastern Indian Ocean to Pacific Ocean, thus inducing a La Niña-like state in the Pacific Ocean.

Figure 4 plots the subsurface temperature anomalies in the equatorial vertical section of the Pacific Ocean. It clearly shows that cold subsurface sea temperature anomalies first appear in the western Pacific in Aug(0), as a result of ITF anomalies. These cold anomalies then propagate into the eastern Pacific, maintaining a La Niña-like cooling state until the following year. The propagation of these cold subsurface temperature anomalies also suggests a role of the ITF during positive IOD forcing, leading to an influence on the following year's La Niña events in the Pacific Ocean.

4.1.2. *Sensitivity experiments forced by CESM1.0.3 atmospheric forcing during positive IOD events*

The observational record associated with IOD events has a short history. Therefore, to further validate the results in section 4.1.1, we use the outputs of the coupled model, CESM1.0.3, to repeat the experiments. A total of 14 positive IOD events (see Fig. 1c) are selected, based on the 100-year time series of SSTAs in the coupled model outputs, and from which the atmospheric forcing fields are extracted. All the sensitivity experiments are completed using the same experimental strategy described in section 4.1.1, except that the climatological and positive IOD atmospheric forcing are extracted from the 100-year time series of the long-term run of CESM1.0.3.

Similar to the results shown in section 4.1.1, negative SSHAs are established in the eastern Indian Ocean in summer, indicating an anomalous upwelling that induces cold temperature anomalies. These upwelling anomalies and SSHAs propagate through the Indonesian seas, giving rise to cold temperature anomalies in the subsurface layer of the tropical western Pacific (Fig. 5). These cold anomalies propagate to the tropical eastern Pacific, where they ultimately dominate and result in a La Niña-like mode in the following year. The cold anomalies in the eastern Pacific Ocean are much weaker than those from the sensitivity experiments using the observed positive IOD forcing. These differences may result from the deficiencies of the coupled model in simulating the IOD strength.

These results demonstrate that, as in the observation, positive IOD events modeled by CESM1.0.3 can influence the

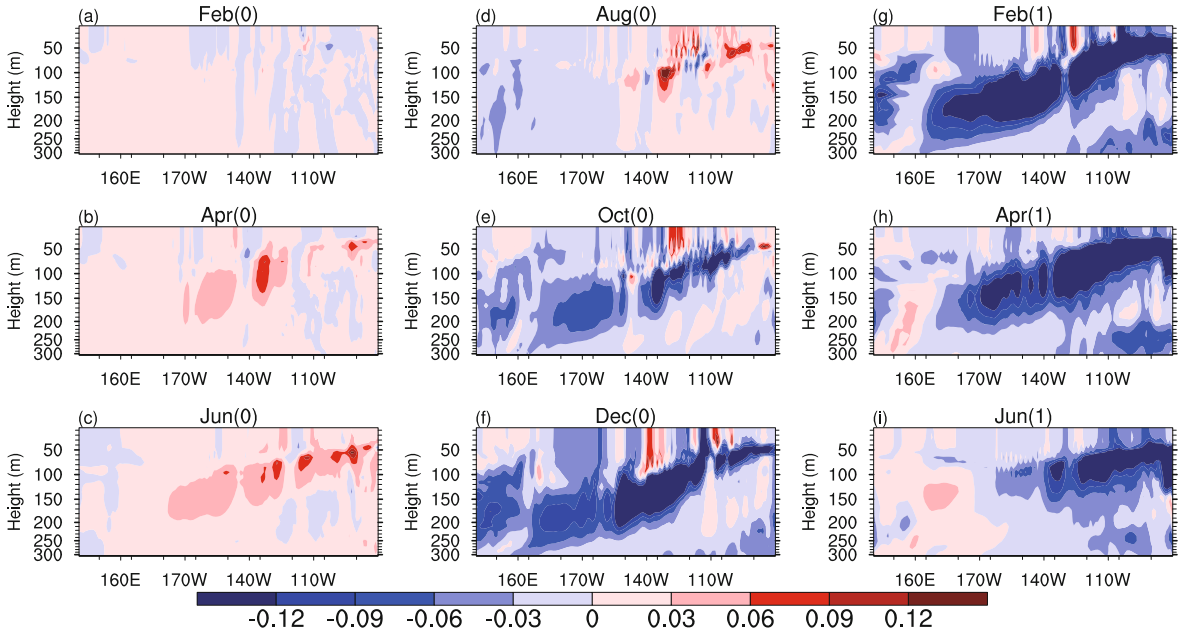

Fig. 4. Composite OGCM-simulated sea temperature anomalies (units: °C) in the equatorial vertical section of the Pacific Ocean between sensitivity experiments forced by observed positive IOD events and the control run during Feb(0) to Jun(1).

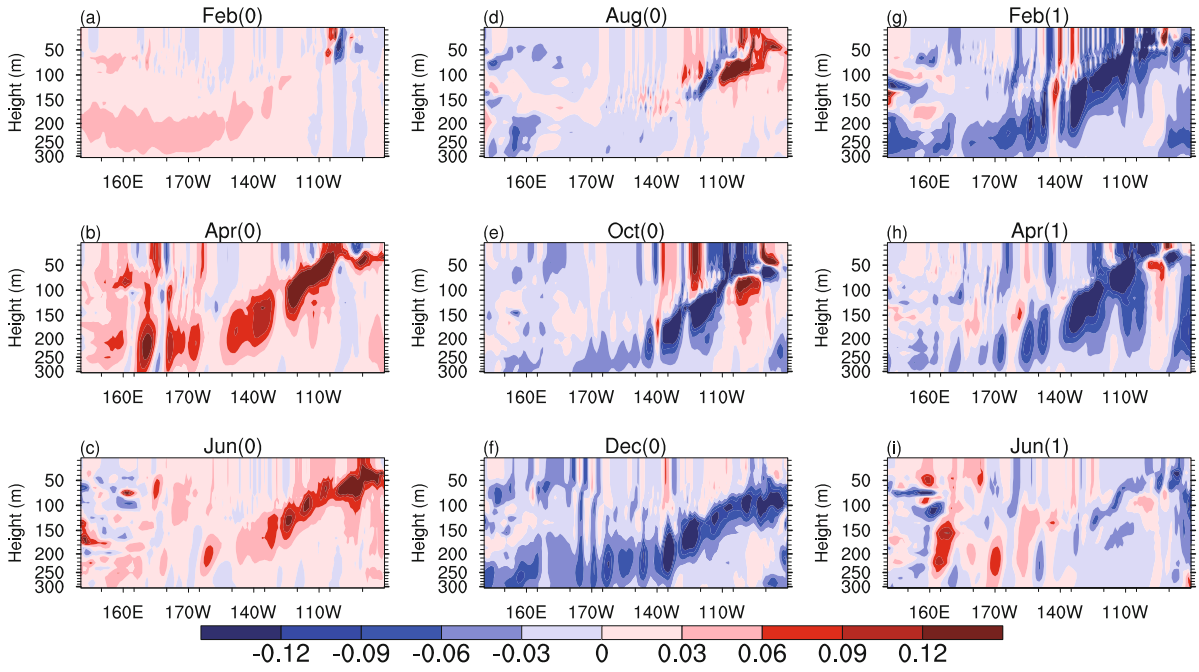

Fig. 5. As in Fig. 4, but for composite temperature anomalies from sensitivity experiments on the 14 positive IOD events from the CESM1.0.3 long-term run.

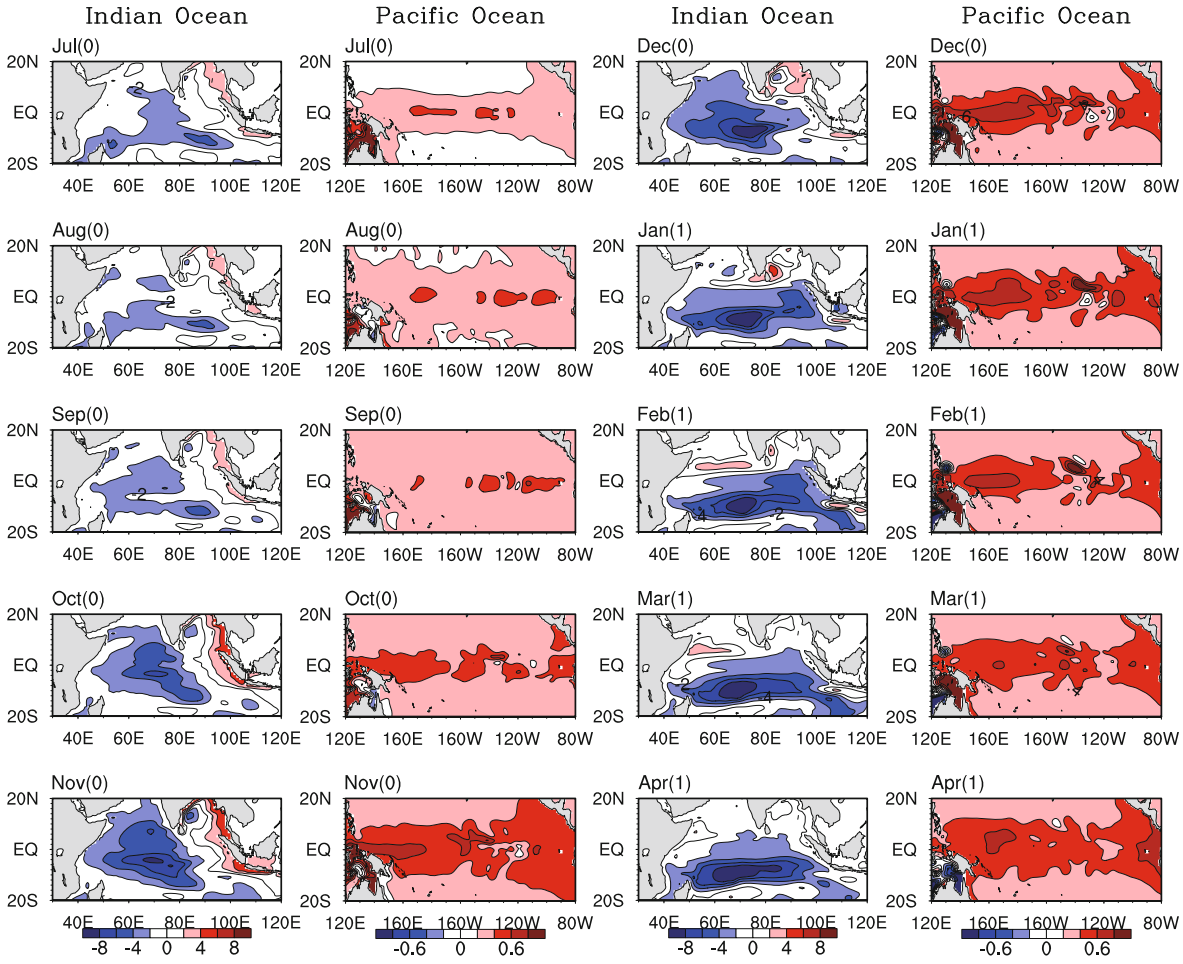

Fig. 6. As in Fig. 2, but for composite SSHAs from sensitivity experiments on negative observed IOD events.

state of the Pacific Ocean in the following year through the tropical ocean channel. This suggests that the role of the ITF in conveying the positive IOD impact on the following year's ENSO is robust.

4.2. *Role of the ITF in the influence of negative IOD on Pacific SST*

As demonstrated in section 4.1, a positive IOD event may induce negative SSHAs in the eastern Indian Ocean. Upwelling anomalies associated with these negative SSHAs propagate across the ITF passages and spread eastward, inducing cold anomalies in the eastern Pacific Ocean and forming La Niña-like SST anomalies in the following year. In this section, we investigate the role of the ITF during negative IOD events in influencing the Pacific SST.

For observed negative IOD events, the design of the sensitivity experiment is the same as that in section 4.1.1, except that the atmospheric forcing in negative IOD years (1975, 1980, 1981, 1989 and 1992) is used as the forcing factor in the experiments. Figure 6 plots the composite SSHAs corresponding to the observed negative IOD events from Jul(0) to Apr(1) over the Indian Ocean and Pacific region. The negative SSHAs in the western Indian Ocean, and the positive anomalies in the east, indicate the existence of a negative IOD. The positive SSHAs in the eastern Indian Ocean suggest an enhancement of the thermocline depth and downwelling signals. These SSHAs and downwelling anomalies get stronger in the following months, propagating into the western Pacific Ocean. The propagation of the positive SSHAs into the Pacific Ocean must take place through the Indonesian seas because the atmospheric bridge is closed in these sensitivity experiments.

The ITF volume and heat flux transport anomalies shown in Fig. 7 further demonstrate the role of the ITF. The negative ITF anomalies during negative IOD events appear in Aug(0), peak in Dec(0), and reverse sign in Mar(1). The negative ITF transport anomalies prove that the downwelling anomalies in the eastern Indian Ocean propagate from the Indian Ocean to the western Pacific Ocean. These downwelling anomalies further induce an El Niño-like state in the Pacific Ocean, which can be traced from the sea temperature anomalies in the vertical section of the equatorial Pacific Ocean (see Fig. 8). This shows that in the tropical Pacific Ocean, warm subsurface sea temperature anomalies appear in the western part, as a result of ITF transport anomalies. These warm anomalies then propagate to the eastern Pacific, maintaining an El Niño-like warming state through to the next year.

Similar to the analysis of positive IOD events, further sensitivity experiments are conducted to examine the role of the ITF in the influence of negative IOD on the Pacific Ocean (Fig. 9), but with the atmospheric forcing provided by 14 negative IOD events from the CESM1.0.3 coupled long-term run (Fig. 1c). The results correlate closely with the observed atmospheric forcing. Therefore, we conclude that negative IOD events can influence ENSO via the ITF, leading to an El Niño-like state in the tropical Pacific Ocean in the following year.

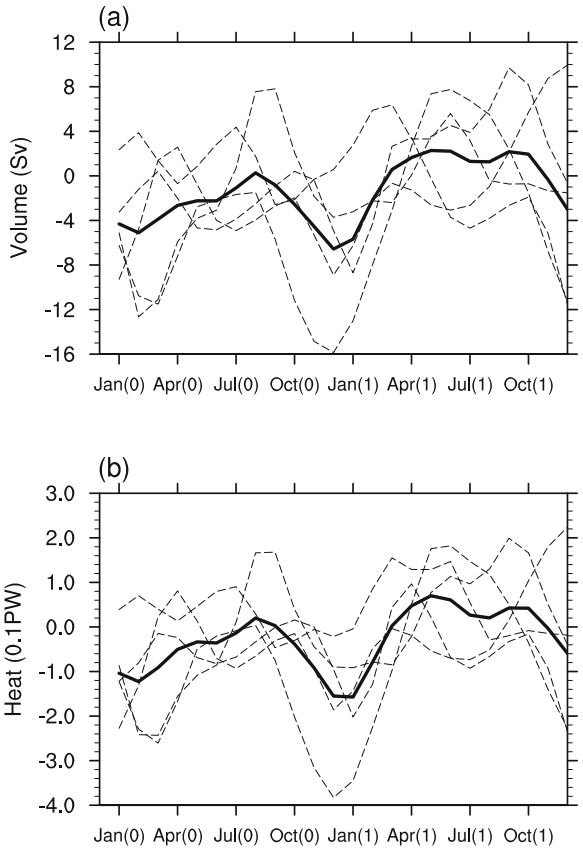

Fig. 7. As in Fig. 3, but for the ITF anomalies from sensitivity experiments on negative observed IOD events.

5. Estimation of the contribution of IOD forcing to the Pacific variability associated with ENSO

In this study, the role of the ITF in the influence of both positive and negative IOD forcing on ENSO is explored. Specifically, positive IOD forcing in the tropical Indian Ocean can result in negative SSHAs in the eastern Indian Ocean. These negative SSHAs pass through the Indonesian seas and lead to a La Niña-like state in the eastern Pacific Ocean the following year. For negative IOD forcing, positive SSHAs appear in the eastern Indian Ocean and propagate into the western Pacific Ocean through the ITF, and then these positive SSHAs ultimately induce an El Niño-like state the following year. We notice that the SSHAs excited by the IOD forcing in the Indian Ocean are significantly reduced when entering the Pacific Ocean (see Figs. 2 and 6). Consequently, we wonder to what extent the IOD forcing contributes to the Pacific variability associated with ENSO.

To address this question, we calculate the SSHAs in the Indian and Pacific oceans under the uncoupled configuration, and compare them with the SSH standard deviation under the coupled configuration to estimate the contribution of the IOD forcing to the ENSO-related Pacific variability. We first calculate the SSH standard deviation in the Indian and Pacific

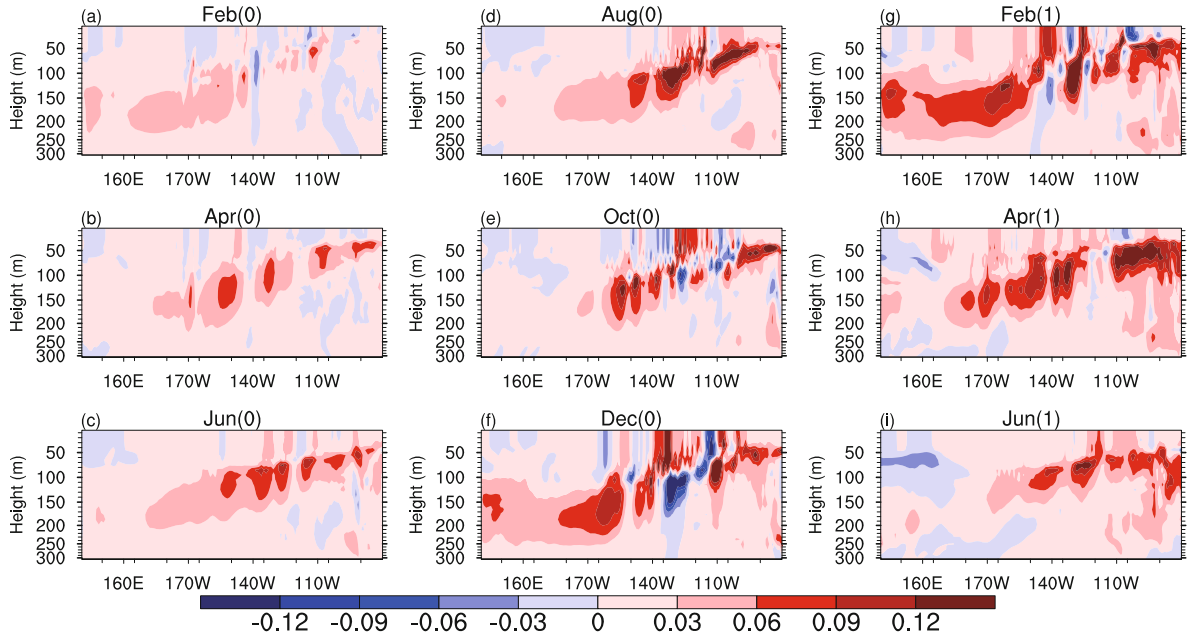

Fig. 8. As in Fig. 4, but for composite temperature anomalies from sensitivity experiments on negative observed IOD events.

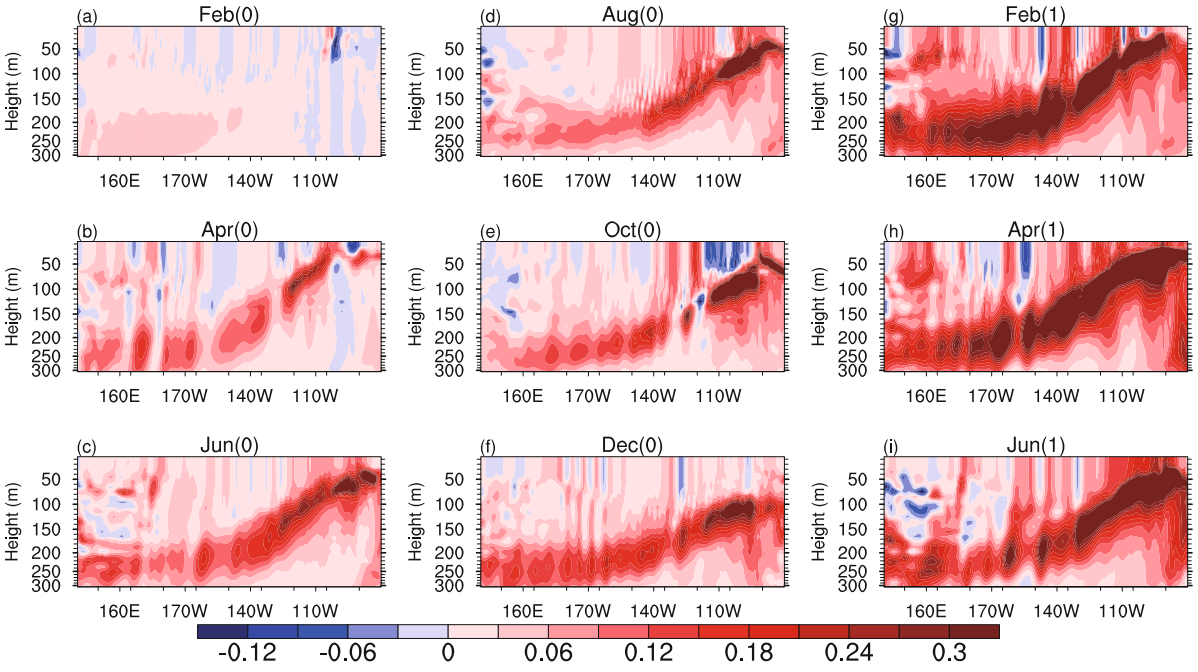

Fig. 9. As in Fig. 4, but for composite temperature anomalies from sensitivity experiments on 14 negative IOD events from the CESM1.0.3 long-term run.

oceans in terms of the CESM1.0.3 output in the model years 0051 to 0150, and the observations (TOPEX/POSEIDON) during the period 1980–2008. Since IOD events often peak in boreal autumn and the SSH variability may have a much larger influence on the tropical Pacific Ocean via the ITF, we plot the SSH standard deviation in this season (exactly in November), derived from both CESM1.0.3 and observations, in Figs. 10a and b. The results indicate that the model goes some way toward representing the true situation, such that it can be used to estimate the contribution of the IOD forcing to the ENSO-related Pacific variability through the ITF. Meanwhile, since the SSHAs in the eastern Indian Ocean can indicate the propagation of Indian Ocean anomalies to the Pacific through the ITF (see section 4), and the SSHAs in the eastern Pacific Ocean are closely related to ENSO, we further calculate the SSH standard deviation in the eastern Indian Ocean

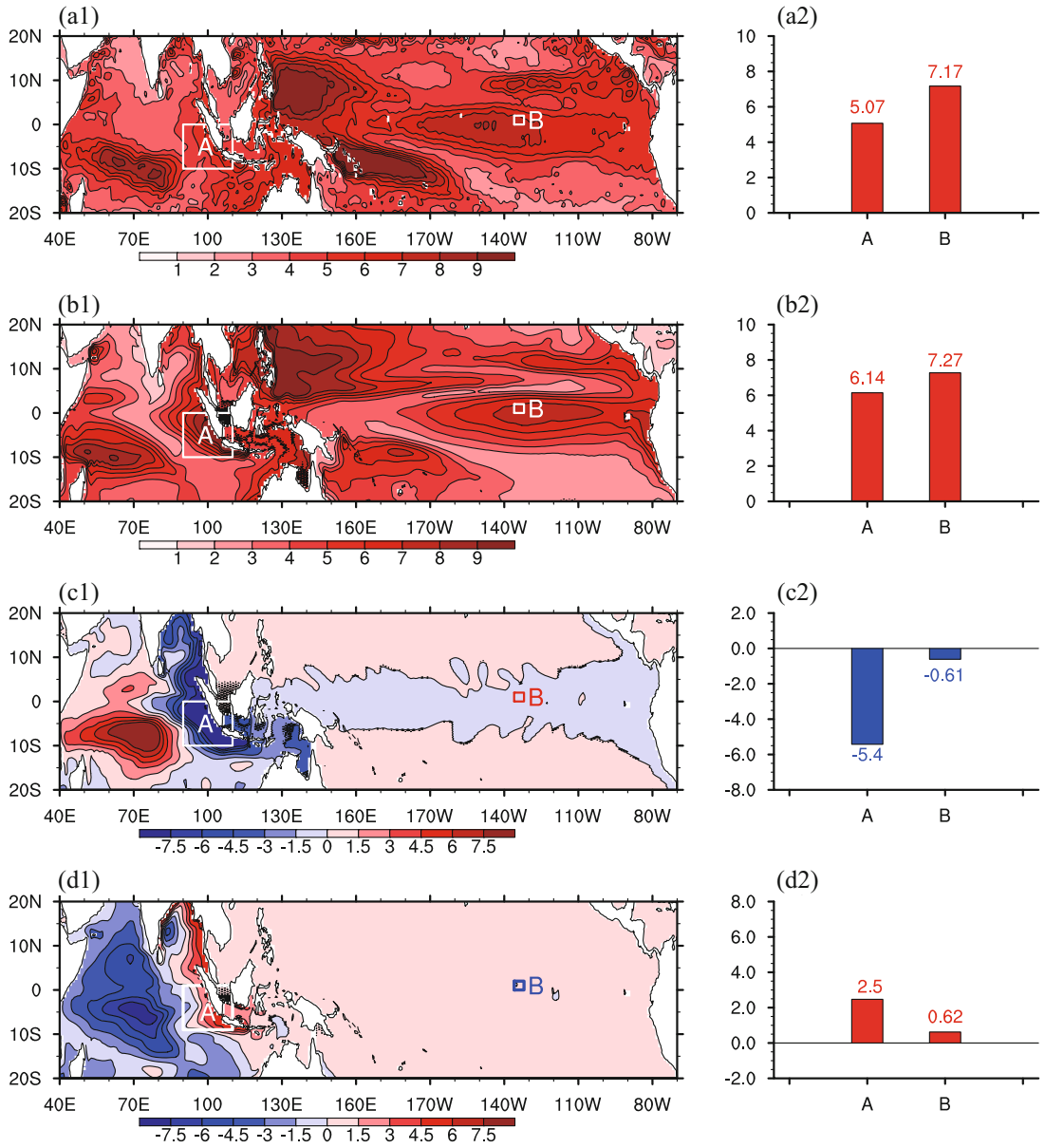

Fig. 10. The SSH standard deviation (units: cm) in November from (a1) observations (TOPEX/POSEIDON) and (b1) the coupled model CESM1.0.3. The ensemble mean of the SSHAs induced by the (c1) observed positive IOD forcing, and (d1) negative IOD forcing in sensitivity experiments. Panels (a2–d2) represent the averaged SSHA values (units: cm) over regions A and B.

and eastern Pacific Ocean (represented by regions A and B in Fig. 10, where the SSHAs are shown to be largest) in November. Results for regions A and B also indicate that the model closely reproduces the observed situation. It is conceivable that, if only IOD forcing over the Indian Ocean is considered and the atmospheric forcing over the Pacific Ocean is the climatological state, then the change of the Pacific variability associated with ENSO may solely depend on the IOD forcing via the ITF. Therefore, SSHAs in region B under the uncoupled configuration and the SSH standard deviation under the coupled configuration can be compared to estimate the contribution of the IOD forcing to the Pacific variability associated with ENSO.

Figures 10c1 and 10d1 plot the ensemble means of the SSHAs during Nov(0) composited from all the observed positive and negative IOD forcings used in this study. For positive IOD forcing, during Nov(0), when positive IOD events peak, the ensemble mean of the SSHAs in region A is about -5.4 cm, which is roughly equal to the SSH standard deviation there; while in region B, the ensemble mean of the SSHAs is -0.61 cm. Quantitatively, positive IOD forcing in the Indian Ocean may explain about 8% (0.61 cm divided by 7.27 cm) of the SSHAs in the eastern Pacific. For negative IOD forcing, it is shown in Figs. 10d1 and 10d2 that negative IOD forcing can also explain about 8% of the El Niño-related SSHAs in the eastern Pacific through the ITF.

We notice that the sensitivity experiments shown in Figs. 10c and 10d tend to underestimate the SSHAs in the eastern Indian Ocean. Correspondingly, the SSHAs in the eastern Pacific might also be underestimated. Despite this, the small SSHAs in the eastern Pacific induced by the IOD forcing in the Indian Ocean could also exhibit significant growth due to the air–sea interaction in the tropical Pacific Ocean, and thereby greatly influence ENSO.

6. Summary and discussion

We use the oceanic model POP2, with observed and coupled-model-simulated external forcing from positive and negative IOD atmospheric data, to conduct sensitivity experiments to examine the role of the ITF in the influence of the IOD on ENSO.

The results demonstrate that positive IOD events, both observed and modeled, can influence (via the ITF) the SSTAs associated with ENSO in the tropical eastern Pacific, inducing a La Niña-like state in the Pacific Ocean the next year. Upwelling anomalies in the eastern Indian Ocean, indicated by negative SSHAs, can penetrate into the western Pacific Ocean through Indonesian sea passages. These SSHAs propagate further eastward, inducing cooling in the eastern Pacific Ocean the following year. These results are in accordance with those of the 1997 positive IOD event obtained by Yuan et al. (2011).

We further investigate the role of the ITF in the influence of negative IOD on ENSO. We demonstrate that negative IOD events can also influence the Pacific Ocean in the following year through the ITF. Physically, downwelling anomalies in the eastern Indian Ocean, reflected by positive SSHAs during negative IOD events, propagate via the ITF into the western Pacific Ocean. These anomalies can further induce warm anomalies in the subsurface of the western Pacific and propagate eastward to the surface of the eastern Pacific. Ultimately, they result in an El Niño-like SSTA state. Therefore, it is clear that the mechanism of the influence of negative IOD on the Pacific Ocean in the following year is symmetrical to that of positive IOD.

We also estimate the contribution of IOD forcing to the ENSO-related Pacific variability. About 8% of the eastern Pacific SSH variability associated with ENSO can be attributed to the IOD forcing in the tropical Indian Ocean through the ITF. However, this result may be dependent on the model we used. More sensitivity experiments carried out using different models is recommended.

Finally, we note that the ITF is a complex passage involving three major channels: the Lombok Strait, the Ombai Strait, and the Timor Sea. The current level of knowledge about these channels limits our understanding of the ITF transportation mechanism. In this study, we simply treat the ITF as a "black box" and do not consider how the upwelling and downwelling anomalies propagate from the Indian to the Pacific Ocean.

Acknowledgements. The authors appreciate the anonymous reviewers very much for their valuable comments and suggestions. This work was sponsored by the National Public Benefit (Meteorology) Research Foundation of China (Grant No. GYHY 201306018).

REFERENCES

Alexander, M. A., I. Blade, M. Newman, J. R. Lanzante, N. C. Lau, and J. D. Scott, 2002: The atmospheric bridge: The influence of ENSO teleconnections on air–sea interaction over the global oceans. *J. Climate*, **15**, 2205–2231.

Allan, R. J., and Coauthors, 2001: Is there an Indian Ocean dipole and is it independent of the El Niño-Southern Oscillation? International CLIVAR Project Office, 18–22.

Annamalai, H., S. P. Xie, J. P. McCreary, and R. Murtugudde, 2005: Impact of Indian Ocean sea surface temperature on developing El Niño. *J. Climate*, **18**, 302–319.

Baquero-Bernal, A., M. Latif, and S. Legutke, 2002: On Dipole-like variability of sea surface temperature in the tropical Indian Ocean. *J. Climate*, **15**, 1358–1368.

Behera, S. K., J. J. Luo, S. Masson, S. A. Rao, H. Sakuma, and T. Yamagata, 2006: A CGCM study on the interaction between IOD and ENSO. *J. Climate*, **19**, 1688–1705.

Chen, D., M. A. Cane, A. Kaplan, S. E. Zebiak, and D. Huang, 2004: Predictability of El Niño over the past 148 years. *Nature*, **428**, 733–736.

Clarke, A. J., and S. Van Gorder, 2003: Improving El Niño prediction using a space-time integration of Indo-Pacific winds and equatorial Pacific upper ocean heat content. *Geophys. Res. Lett.*, **30**, 1399, doi: 10.1029/2002GL016673.

Danabasoglu, G., and Coauthors, 2011: The CCSM4 ocean component. *J. Climate*, **25**, 1361–1389.

Deser, C., and Coauthors, 2012: ENSO and Pacific decadal variability in the community climate system model version 4. *J. Climate*, **25**, 2622–2651.

Diaz, H. F., M. P. Hoerling, and J. K. Eischeid, 2001: ENSO variability, teleconnections and climate change. *International Journal of Climatology*, **21**, 1845–1862.

Hong, C.-C., T. Li, and J.-J. Luo, 2008a: Asymmetry of the Indian Ocean dipole. Part II: Model diagnosis. *J. Climate*, **21**, 4849–4858.

Hong, C.-C., T. Li, L. Ho, and J.-S. Kug, 2008b: Asymmetry of the Indian Ocean dipole. Part I: Observational analysis. *J. Climate*, **21**, 4834–4848.

Izumo, T., M. Lengaigne, J. Vialard, J. J. Luo, T. Yamagata, and G. Madec, 2014: Influence of Indian Ocean Dipole and Pacific recharge on following year's El Niño: Interdecadal robustness. *Climate Dyn.*, **42**, 291–310.

Izumo, T., and Coauthors, 2010: Influence of the state of the Indian Ocean Dipole on the following year's El Niño. *Nature Geoscience*, **3**, 168–172.

Jin, E., and Coauthors, 2008: Current status of ENSO prediction skill in coupled ocean–atmosphere models. *Climate Dyn.*, **31**, 647–664.

Jochum, M., B. Fox-Kemper, P. H. Molnar, and C. Shields, 2009: Differences in the Indonesian seaway in a coupled climate model and their relevance to Pliocene climate and El Niño. *Paleoceanography*, **24**, PA1212, doi: 10.1029/2008PA 001678.

Kug, J. S., and I. S. Kang, 2006: Interactive feedback between ENSO and the Indian Ocean. *J. Climate*, **19**, 1784–1801.

Large, W. G., and G. Danabasoglu, 2006: Attribution and impacts of upper-ocean biases in CCSM3. *J. Climate*, **19**, 2325–2346.

Latif, M., and Coauthors, 1998: A review of the predictability and prediction of ENSO. *J. Geophys. Res.:-Oceans*, **103**, 14375–14393.

Lau, N.-C., and M. J. Nath, 2003: Atmosphere–Ocean Variations in the Indo-Pacific Sector during ENSO Episodes. *J. Climate*, **16**, 3–20.

Lee, T., and Coauthors, 2010: Consistency and fidelity of Indonesian-throughflow total volume transport estimated by 14 ocean data assimilation products. *Dyn. Atmos. Oceans*, **50**, 201–223.

Luo, J.-J., S. Masson, S. K. Behera, and T. Yamagata, 2008: Extended ENSO predictions using a fully coupled ocean–atmosphere model. *J. Climate*, **21**, 84–93.

Luo, J.-J., R. Zhang, S. K. Behera, Y. Masumoto, F.-F. Jin, R. Lukas, and T. Yamagata, 2010: Interaction between El Niño and Extreme Indian Ocean Dipole. *J. Climate*, **23**, 726–742.

Meng, W., and G. X. Wu, 2000: Gearing between the Indian and Pacific Ocean (GIP) and the ENSO, Part 2. model simulation. *Chinese Journal of Atmospheric Sciences*, **24**, 15–25. (in Chinese)

Meyers, G., R. J. Bailey, and A. P. Worby, 1995: Geostrophic transport of Indonesian Throughflow. *Deep-Sea Research Part I-Oceanographic Research Papers*, **42**, 1163–1174.

Nagura, M., and M. Konda, 2007: The seasonal development of an SST anomaly in the Indian Ocean and its relationship to ENSO. *J. Climate*, **20**, 38–52.

Nicholls, N., W. Drosdowsky, and A. M. S. Ams, 2001: Is there an equatorial Indian Ocean SST dipole, independent of the El Niño-Southern Oscillation? Climate Variability, the Oceans, and Societal Impacts, *The The 81st AMS Annual Meeting,* Albuquerque, NM, U.S., January 2001, 17–18.

Roxy, M., S. Gualdi, H. K. L. Drbohlav, and A. Navarra, 2011: Seasonality in the relationship between El Niño and Indian Ocean dipole. *Climate Dyn.*, **37**, 221–236.

Saji, N. H., and T. Yamagata, 2003: Structure of SST and surface wind variability during Indian Ocean dipole mode events: COADS observations. *J. Climate*, **16**, 2735–2751.

Schott, F. A., S. P. Xie, and J. P. McCreary Jr., 2009: Indian ocean circulation and climate variability. *Rev. Geophys.*, **47**, doi: 10.1029/2007RG000245.

Shinoda, T., W. Han, E. J. Metzger, and H. E. Hurlburt, 2012: Seasonal Variation of the Indonesian Throughflow in Makassar Strait. *J. Phys. Oceanogr.*, **42**, 1099–1123.

Tippett, M. K., A. G. Barnston, and S. Li, 2011: Performance of recent multimodel ENSO forecasts. *J. Appl. Meteor. Climatol.*, **51**, 637–654.

Wang, B., R. G. Wu, and X. H. Fu, 2000: Pacific–East Asian teleconnection: How does ENSO affect East Asian climate? *J. Climate*, **13**, 1517–1536.

Wu, G., and W. Meng, 1998: Gearing between the Indian and Pacific Ocean (GIP) and the ENSO, Part 1. Data analyses. *Chinese Journal of Atmospheric Sciences*, **22**, 470–480. (in Chinese)

Wyrtki, K., 1987: Indonesian through flow and the associated pressure gradient. *J. Geophys. Res.: Oceans*, **92**, 12941–12946.

Yuan, D. L., and Coauthors, 2011: Forcing of the Indian Ocean Dipole on the interannual variations of the tropical Pacific Ocean: Roles of the Indonesian Throughflow. *J. Climate*, **24**, 3593–3608.

Yuan, D. L., H. Zhou, and X. Zhao, 2013: Interannual climate variability over the tropical Pacific Ocean induced by the Indian Ocean Dipole through the Indonesian Throughflow. *J. Climate*, **26**, 2845–2861.